energies

MDPI

Article

Assessing the Techno-Economic Impact of Derating Factors on Optimally Tilted Grid-Tied Photovoltaic Systems

Hasan Masrur [1,*], Keifa Vamba Konneh [1], Mikaeel Ahmadi [1], Kaisar R. Khan [2], Mohammad Lutfi Othman [3] and Tomonobu Senjyu [1]

[1] Department of Electrical & Electronics Engineering, Faculty of Engineering, University of the Ryukyus, 1 Senbaru, Nishihara-cho, Nakagami, Okinawa 903-0213, Japan; k208677@eve.u-ryukyu.ac.jp (K.V.K.); k188684@eve.u-ryukyu.ac.jp (M.A.); b985542@tec.u-ryukyu.ac.jp (T.S.)
[2] Eversource Energy, Southborough, Boston, MA 02090, USA; kaisar@knights.ucf.edu
[3] Advanced Lightning and Power Energy Research (ALPER), Department of Electrical and Electronic Engineering, Faculty of Engineering, Universiti Putra Malaysia, Seri Kembangan 43400, Selangor, Malaysia; lutfi@upm.edu.my
* Correspondence: k198676@eve.u-ryukyu.ac.jp or hmasrur@gmail.com

Abstract: Photovoltaic (PV) systems encounter substantial losses throughout their lifespan due to the different derating factors of PV modules. Those factors mainly vary according to the geographical location and PV panel characteristics. However, the available literature does not explicitly concentrate on the technical and economic impact of the derating factors within the PV system. Owing to that necessity, this study performs a comprehensive analysis of various PV loss parameters followed by a techno-economic assessment of derating factors using the average value on a grid-connected and optimally tilted PV system located in Hatiya, Bangladesh. Some criteria linked to the derating factors such as PV degradation and ambient temperature are further explored to analyze their impact on the aforementioned power system. Simulation results show that PV power generation would vary around 12% annually, subject to a 10% variation in the derating factor. Again, a 10% difference in the derating factor changes the net present cost (NPC) by around 3% to 4%. The system provides the best technical performance concerning annual PV production, power trade with the grid, and the renewable fraction at a higher value of the derating factor since it represents a lower impact of the loss parameters. Similarly, the financial performance in terms of the NPC, levelized cost of energy (LCOE), and grid power exchange cost is found to be lower when the derating factor value is higher.

Keywords: PV derating factor; techno-economic analysis; grid-tied PV; simulation and optimization

Citation: Masrur, H.; Konneh, K.V.; Ahmadi, M.; Khan, K.R.; Othman, M.L.; Senjyu, T. Assessing the Techno-Economic Impact of Derating Factors on Optimally Tilted Grid-Tied Photovoltaic Systems. *Energies* **2021**, *14*, 1044. https://doi.org/10.3390/en14041044

Academic Editor: Ignacio Mauleón
Received: 8 January 2021
Accepted: 9 February 2021
Published: 17 February 2021

1. Introduction

Solar power has recently seen the biggest rise in its share among renewable energy technologies. As a matter of fact, in 2017, the installed power capacity of solar PV even dominated the combination of nuclear, coal, and gas, which proves the significant impact of solar energy on current power generation and total final energy consumption [1]. The price of PV modules is declining rapidly, leading to the reduction of the LCOE of PV electricity. It is reported that within eight years (2010–2018), the LCOE of solar PV has decreased by 77% [2]. However, one of the main setbacks that the PV systems face is the different derating parameters caused by weather conditions and the PV modules themselves. Were their techno-economic effect properly realized, the progress of these PV projects could surely accelerate further.

The derating factor of PV modules is the combination of different loss parameters that reduce the PV output power. Some derating factors are reversible (e.g., soiling can be reversed by cleaning the modules) or irreversible (e.g., material degradation can rarely be reversed). An example of the typical values commonly assumed for PV system losses [3] are shown in Table 1; the values may vary according to the climatic conditions. Apart from

these, the power conditioning unit (inverter), transformers, and sun-tracking also affect the AC power rating of the grid-coupled PV system [4]. However, the existing literature mostly discusses the technical effect of the derating factors on the PV system [5–13]. Very few studies are available pointing out the economic effect of a single derating factors such as soiling, shading, and degradation along with the technical impact [14–19].

PV modules face notable power loss because of soiling. Any form of dust, dirt, snow, bird droppings, biofilms of bacteria, pollen, and other particles that cover the PV module surface can be considered as soiling [11,16]. A study in Pakistan by Ullah et al. [6] investigated the soiling effect of solar modules and found out that soiling can cause a 10% PV output power loss in the case of lightly soiled panels, and it could go up to 40% for heavily stained panels. The authors in [20] recommended that 5% of the derating value should be assigned while designing a PV project based on their findings on energy losses for two different climatic conditions of Australia and Indonesia. You et al. [21] examined the techno-economics of a soiled PV module across seven cities and found that cleaning interval has a substantial impact on the net present value (NPV) of the PV system. Reference [7] took into account almost all derating factors such as high temperature, cloud, aerosol optical depth, high dust concentration, snow, shadow, etc., to examine the performance of a 720Wp PV system. Rainfall plays a vital role in removing soiling from the PV panels, as pointed out by several studies [9–11], which eventually improves the PV output efficiency. Dirt and dust can be cleaned in the rainy season in Bangladesh, but this period is has been decreasing recently. Typically, in rural areas of Bangladesh, including the study area, there is much dust during the dry season. Hence, soiling is an essential factor in calculating the PV efficiency; in fact, Rahman et al. [13] indicated that solar PVs, located in the Bangladeshi environment, can lose their effectiveness by up to 35% in a month due to the accumulated dust. Typically, PV modules have a lower derating factor value in the summer season than winter because of the losses associated with the higher PV cell temperature. If soiling is seasonal, then the value can also change from the dry to the rainy season. As a matter of fact, Micheli et al. [22] stated that a PV system could encounter more than a 20% power drop due to seasonal soiling where the yearly soiling losses were limited to only 3%.

PV degradation refers to the gradual declination of the power output of the PV module over time. Known also as aging, the degradation rate plays a crucial role in the PV industry as it affects the investment decision for a PV related project [23]. Several factors will accelerate the aging process of the PV panel, for example PV panels themselves, the PV design process, climatic conditions, UV, temperature, and so on. However, it is not very easy to find the exact life-cycle of PV panels since each panel has its own aging evolution [12]. According to a recent study in Thailand, the PV degradation rate ranged between 0.3 and 1.9%/year, resulting in a 4.1 to 14 baht/kWh levelized cost of electricity (LCOE) [24]. Non-linear degradation is also crucial as it directly affects the LCOE [25]. In fact, Reference [26] proposed a methodology that displayed 6.14% differences in LCOE compared to existing methods. Article [27] argued that non-linear degradation affects the cleaning of PV panels as well. Quansah et al. [19] studied the techno-economics of the degradation rate of PV panels exposed for sixteen years to the sunny northern Ghanaian atmosphere. According to their investigation, PV modules degraded non-linearly at an annual rate of 1.54%, and at an average end-user tariff of \$0.2/kWh, the PV project is worthy of further investment. PV mismatch and wiring loss are critical parameters of the derating factor as well since they can contribute to around a 2–3% loss in the PV system [28]. Another imperative parameter that decreases PV output power is DC to AC conversion. Figure 1 demonstrates a graphical presentation of some derating parameters, and Figure 2 shows a typical derated PV panel.

Table 1. PV system losses [3].

Loss Parameters	Value (%)
Soiling	2
Shading	3
Mismatch	2
Wiring	2
Connections	0.5
Light-induced degradation	1.5
Nameplate rating	1
Availability	3

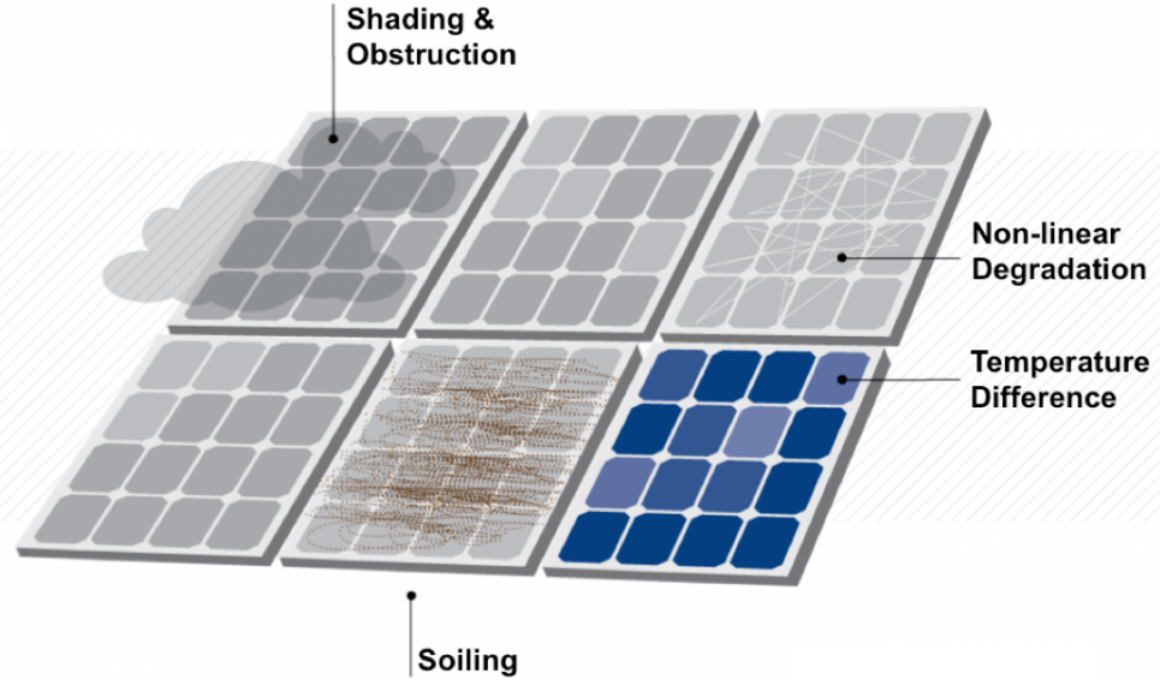

Figure 1. Graphical presentation of different derating parameters [29].

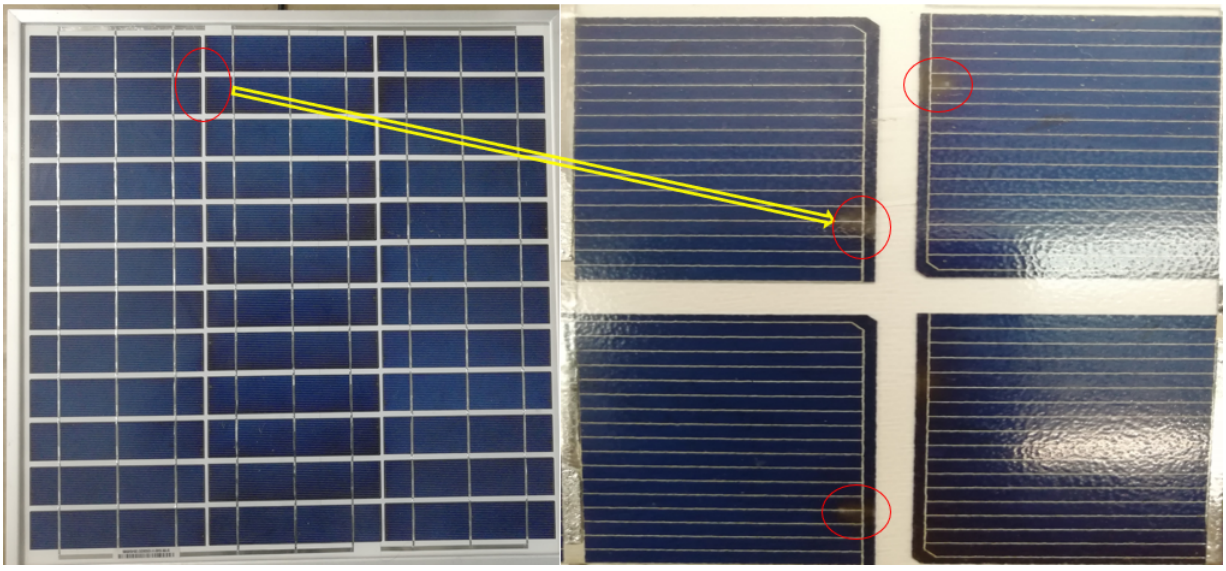

Figure 2. A typical derated PV panel.

Many researchers pointed out the techno-economic impact of unique geographic location, sun-tracking, tilt angle, azimuth, and ambient temperature on PV-based systems. However, very few have discussed the techno-economic-environmental impact of the derating factors. Table 2 summarizes the findings from the selected PV-focused literature considering different characteristics relevant to solar power and photovoltaic technology. It also highlights the features of the current study.

Highlighting mainly standalone hybrid PV systems, a handful studies are available on the grid-connected PV systems of Bangladesh, with zero discussion of the techno-economics of PV derating factors. For example, Mondol et al. [30] proposed and examined the feasibility of a 1 MW grid-tied solar power plant. Assuming the load data, the study showed favorable conditions, sites, and indicators for the presented system. The proposed grid-integrated solar PV system by Arif et al. [31] in the southeastern part of Bangladesh indicated the economic and environmental suitability of the selected site. Shuvo et al. [32] carried out a technical investigation on the prediction of solar energy and the performance of an 80 kWp grid-tied PV plant. They concluded that the artificial neural network (ANN) forecasts solar irradiation better than fuzzy logic, which eventually assists in designing efficient solar PV projects. Similarly, Reference [33] analyzed the feasibility of a PV-based system for irrigation without considering any PV loss factors.

Table 2. Summary of selected PV-focused energy systems in the literature.

Ref.	System Configuration	Grid Connection	Optimization and Sensitivity Analysis Considering PV Related Features									Optimization Criteria	Optimization Tool/Method
			Different Climate /Solar Radiation	Tracking	Tilt Angle	Azimuth	MPPT	Temperature	Derating Factor	Ground Reflectance	Lifetime		
This Study	PV	✓	-	✓	-	-	-	✓	✓	✓	✓	T^a/E^b	HOMER
Ref. [34]	Wind-PV -Battery	-	-	-	✓	-	-	✓	-	-	-	T/E	HOMER
Ref. [5]	PV-Diesel	-	✓	-	✓	✓	-	✓	-	-	-	T/E	HOMER
Ref. [15]	PV-PSH	-	-	✓	-	-	-	-	-	-	-	T/E	NSGAII
Ref. [18]	PV-Wind	-	-	✓	✓	-	-	-	-	-	-	T/E	HOMER
Ref. [14]	PV	✓	-	✓	-	-	-	-	-	-	-	T/E	HOMER
Ref. [35]	PV-Battery	-	-	✓	✓	-	-	-	-	-	-	$T/E/V^c$	HOMER
Ref. [36]	PV-Diesel	-	✓	-	-	-	-	-	-	-	-	T/E/V	HOMER
Ref. [37]	PV-Wind	✓	-	-	✓	-	-	-	-	-	-	T	GA
Ref. [6]	PV	-	-	-	✓	-	-	-	✓	-	-	T	MATLAB
Ref. [38]	PV	✓	-	-	-	-	-	-	-	-	-	T/E	DER-CAM
Ref. [39]	PV-Diesel -Storage	✓	-	-	-	-	-	-	-	-	-	T/E	DER-CAM
Ref. [7]	PV	-	-	-	-	-	-	✓	✓	-	-	T	Experimental
Ref. [40]	PV-Battery -Hydrogen	✓	-	-	-	-	-	-	-	-	✓	T/E	ODYSSEY
Ref. [8]	PV	-	-		-	-	-	-	✓	-	-	T	Experimental
Ref. [41]	PV-Wind -Diesel-battery	-	✓	-	-	-	-	-	-	-	-	E	HOMER
Ref. [42]	PV-Wind -Battery	-	✓	-	-	-	-	-	-	-	-	E	HOMER
Ref. [43]	PV	✓	-	-	-	-	-	-	-	-	-	T/E/V	PSO
Ref. [44]	PV	-	-	-	-	-	✓	-	-	-	-	T	PSO
Ref. [45]	PV-Wind	-	-	-	-	-	-	-	-	-	-	T/E	NSGA-II
Ref. [46]	PV	✓	-	-	✓	-	-	-	-	-	-	T/E	GA

T^a = technical, E^b = economic, and V^c = environmental.

In light of the earlier discussion, the objective of this study is to propose and investigate a decentralized grid-connected community rooftop PV system considering the influence of different loss parameters (derating factor) in terms of technical and economic criteria. It aims to find the best derating factor for the PV module, which would yield efficient PV power with lower investment cost when tied to the grid.

The contributions of this study can be stated as follows:

- Several works were performed to analyze the influence of PV loss parameters on the technical and financial performance of PV systems, but those were done separately and specifically for a single loss parameter. Again, this has not been extensively

analyzed in the literature, especially for the region in Bangladesh, save this study. A comprehensive table is presented comparing the PV characteristics covered in this study with 20 other existing literature works.

- Furthermore, the study intends to help other countries that share the same climatic conditions to design and apply their PV projects both off-grid and grid-tied by reflecting the PV derating factor. Again, the findings from the paper may help the power system planning of various islands where ample solar energy is available and is to be extracted via PV modules.

2. Research Methodology

The success of any project depends on the suitability of technical, as well as financial parameters. The technical issues that need to be monitored for any solar-powered projects include, but are not limited to proper site selection, the appropriate estimation of the solar irradiation and load profile, the choice of efficient PV modules with a suitable tracking system, the derating factor and lifetime of PV modules, the proper setup, maintaining correct PV panel orientation, regular maintenance, and so on. A detailed discussion of the PV derating factor can be found in the next subsection.

The grid-connected PV system can function with or without a battery backup system. For this study, we did not use battery storage. Therefore, the excess energy production from solar PV panels after meeting the primary demand can be sold to the grid at a reasonable price. In this way, the PV system owner can become a prosumer (producer plus consumer) and can reduce its grid dependency. The economic performance of PV-based grid-coupled systems is highly reliant on local resources and supporting policies such as fiscal incentives and net metering [2,47]. Some common, but essential financial indicators are the retail electricity tariff, the net present value (NPV), the payback period, the internal rate of return (IRR), the LCOE, the NPC, the benefit-cost ratio, and the costs related to capital, replacement, and operation and maintenance. The design configuration of grid-connected PV is shown in Figure 3. The proposed research steps with the methodology are shown in Figure 4.

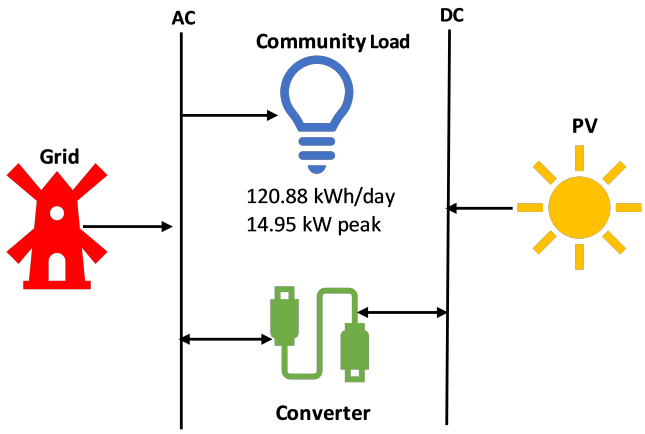

Figure 3. Schematic of the grid-tied PV.

In order to model the PV-grid system and analyze its technical and economic facts, a robust but simple simulation tool is necessary. According to an investigation of Sinha and Chandel [48], the HOMER (Hybrid Optimization Model for Multiple Energy Resources) tool is found to be used widely by researchers. HOMER is well known for its techno-economic modeling and has been used to evaluate energy systems in various climate regions [49]. It takes the technical and cost input of the components along with site-specific meteorological data and delivers the least NPC-optimized hybrid renewable energy system (HRES)configuration after assessing optimal and near optimal values. It allows 1 h time

step data and a wide range of constraints, which makes the design effective and realistic. Therefore, HOMER is used in this paper to carry out the investigation.

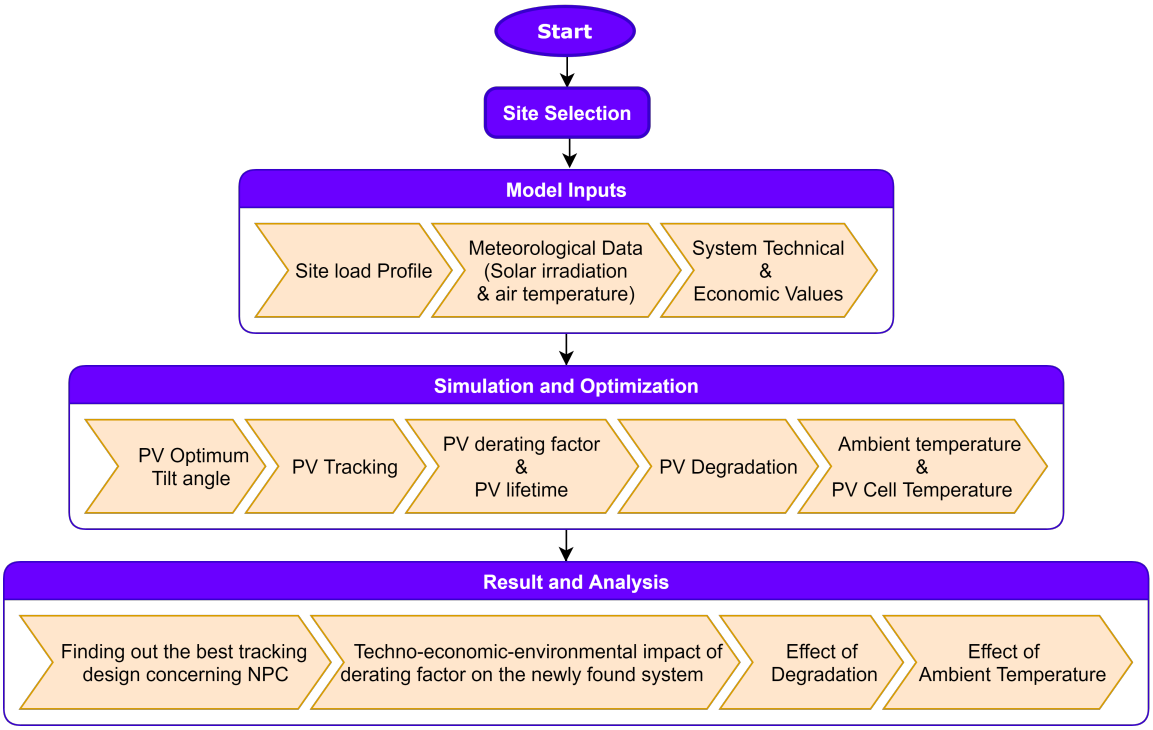

Figure 4. Steps for the overall research methodology.

2.1. Derating Factor

As discussed earlier, derating is a critical factor for the PV module, as it indicates the efficiency of the PV panel. No equipment can produce 100% of its capacity. PV output power can be reduced due to such factors as wiring losses, soiling, snow cover, shading, mismatch, inappropriate diodes and connections, aging, etc. [50]. Initially, we set the PV system power loss at 12%, which results in a derating factor of 0.88 [3] and matches the PV manufacturer's (refer to Table 4) claim. The individual losses assumed in [3] are shown in Table 1. It should be noted that this study has not taken individual derating parameters as the inputs; rather, it merges all and takes one input as a percentage value.

However, the derating factor can be derived from the following formula:

$$D_{PV} = \frac{P_{PV}}{Cp_{PV} * (\frac{Ir}{Ir_{STC}})[1 + \alpha_p(T_c) - T_{c,STC}]} \quad (1)$$

where D_{PV} indicates the derating factor of the solar PV array (%), P_{PV} is the output power from the PV module, Cp_{PV} denotes the rated capacity of the PV array (kW), Ir is the solar irradiation on the PV panel's surface (kW/m^2), Ir_{STC} refers to the incident solar irradiation under standard test conditions (STCs) (1kW/m^2), α_p is the temperature coefficient of power (%/°C), T_c is the PV cell temperature at the present time step (°C), and $T_{c,STC}$ is the PV cell temperature under STCs (25 °C).

From Equation (1), it is evident that apart from the previously mentioned parameters, the derating factor relies on several other factors as well, including cell temperature, which is directly linked to the PV temperature power coefficient (α_p). α_p can vary depending on the PV module type, though normally, it is between −0.20 %/°C and −0.60 %/°C [51]. It has a negative value since the PV output power decreases with the increase of the cell temperature.

Derating factors are heavily dependent on the nature and quality of the PV panels themselves. While normalized performance and losses in a particular area may be the

same for different solar PV array capacities [52], they appear to change with varying locations. With regard to the PV panels, for instance, an amorphous silicon (a-Si) solar panel has a higher degradation rate, while cadmium telluride (CdTe) PV panels have a lower rate. However, in recent years, the performance of PV panels has been getting better due to advanced technology. A detailed discussion on the degradation rates of PV panels can be found in [53]. In this study, we used the mono-crystalline silicon (mono-Si) PV module. It has higher efficiencies than the multi-crystalline (poly-Si) PV panels [54]. Moreover, the article in [55] found that the mono-Si PV module works better than poly-Si in a subtropical monsoon climate like Bangladesh.

2.2. Case Study

For this research, Hatiya (22.2824° N, 91.0969° E) in Bangladesh was selected as the case study. The area is located near the northeastern part of the Indian Ocean called the Bay of Bengal. According to the Köppen-Geiger index, it belongs to the tropical monsoon climate (Am) [56]. Figure 5 shows the map of Hatiya. Being an island and lacking urbanization, Hatiya is exposed to humidity, dust, and other derating parameters that affect PV performance.

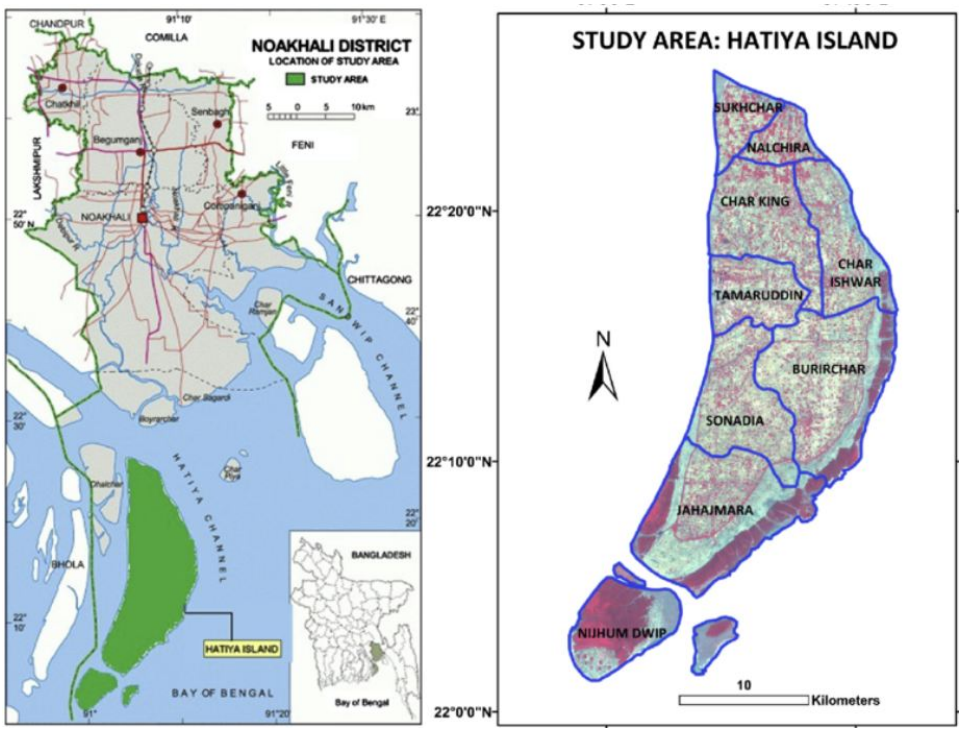

Figure 5. Map of the selected study area.

2.3. Optimum Angle of the PV Panel

Finding the optimal tilt angle for PV panels is crucial to intercept the maximum solar energy and yield the maximum PV power. Since PV tracking systems are expensive, a simple mathematical model can be used to find the optimal angle. In this study, a program was developed in MATLAB to determine the PV panel's optimal angle for Hatiya.

To calculate solar radiation, the following parameters are considered, which were adopted from [57,58]: the GHIvalue from NREL [59] and the latitude of the site; the extraterrestrial radiation (E_0) that falls on the Earth's surface (Equation (2)); the declination angle (δ), which shifts between $-23.45°$ and $23.45°$ (Equation (3)); the solar hour angle, which refers to the deviation between solar noon and local solar time (Equation (4)); and the diffuse solar radiation R_{Df}.

$$E_0 = \frac{24}{\pi} S_0 \left(1 + 0.0033 cos \frac{360n}{365}\right) \quad (2)$$

$$\delta = 23.45^\circ sin\left(\frac{360^\circ}{365}(n + 248)\right) \quad (3)$$

$$w_s = cos^{-1}(-tan\alpha tan\delta) \quad (4)$$

where α is the latitude of Hatiya.

$$R_{Df} = R_G(1.311 - 3.022C_t + 3.427C_t^2 - 1.821C_t^3) \quad (5)$$

when $w_s > 81.4^\circ$.

$$R_{Df} = R_G(1.391 - 3.560C_t + 4.189C_t^2 - 2.137C_t^3) \quad (6)$$

when $w_s < 81.4^\circ$

Here, R_G and C_t refer to the global solar radiation and clearness index, respectively. C_t can be obtained by the following equation:

$$C_t = \frac{R_G}{R_0} \quad (7)$$

In this study, the optimum tilt angle (β) was varied between 0° and 90°. The incident global solar radiation on a tilted surface (R_t) that includes β is calculated by the next equation:

$$R_T = (R_G - R_{Df})E_b + R_G\rho\frac{(1 - cos\beta)}{2} + R_{Df}\frac{(1 - cos\beta)}{2} \quad (8)$$

Here, E_b is a parameter applicable to the surface in the Northern Hemisphere sloped towards the Equator and formulated by the following relation.

$$E_b = \frac{cos(\alpha - \beta)cos\delta sinh_s + h_s sin(\alpha - \beta)sin\delta}{cos\alpha cos\delta sinh_s + h_s sin\alpha sin\delta} \quad (9)$$

where h_s denotes sunset hour angle, derived from the next equation:

$$h_s = min[cos^{-1}(-tan\alpha tan\delta)cos^{-1}(-tan(\alpha + \beta)tan\alpha)] \quad (10)$$

The overall algorithm can be seen in the pseudo-code of Algorithm 1.

The incident solar radiation corresponding to the optimal tilt angle is displayed in Figure 6. The annual average solar radiation was increased from 4.88 kWh/m^2/day to 5.90 kWh/m^2/day after implementing the optimal tilt angle. The difference in terms of the solar radiation and clearness index before and after using β can be found in the Supplementary Materials.

Algorithm 1: Optimization of the PV panel tilt angle.

for Every month **do**
  Consider latitude, global solar radiation, and Julian day
  Vary 0° −90° with a 1° step
  Calculate extraterrestrial radiation (Equation (2)), declination angle (Equation (3)), sunshine hour angle (Equation (4)), and clearness index (Equation (7))
  if $w_s < 0$ **then**
    Calculate R_{Df} using Equation (6)
  else
    Calculate R_{Df} using Equation (5)
  end if
  Calculate R_T using Equation (8) with the support of Equations (9) and (10)
  Find the optimal angle for the maximum R_T
end for

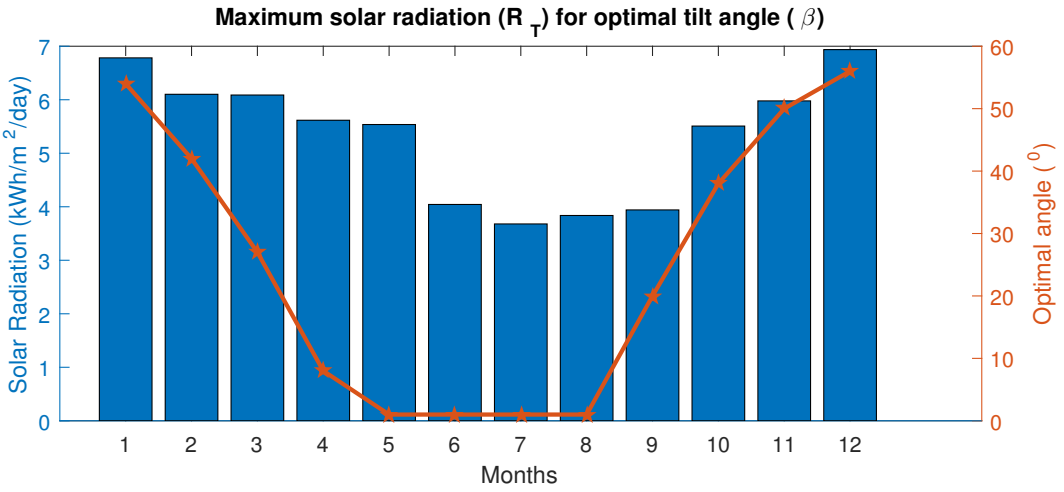

Figure 6. Monthly solar radiation values corresponding to the optimal tilt angle for Hatiya.

2.4. Model Inputs

2.4.1. Meteorological Data

The calculated monthly averaged global solar irradiation and clearness index data incorporating the optimal tilt angle were used as the input. The average annual clearness index was 0.49, and the average daily radiation was 5.90 kWh/m^2/day. The scaled average temperature was rounded up to 25.38 °C.

2.4.2. Grid Tariff

For the sake of simplicity, a simple rate was defined for buying and selling per unit of electricity from and to the grid. Usually, the sell-back price of consumer-produced power is lower compared to the power supplied by the utility grid. This study adopted a flat rate grid power price of 0.094 ($/kWh) and a grid net excess price, i.e., sell-back price of 0.066 ($/kWh) indicated by the Bangladesh Power Development Board (BPDB) [60].

2.5. Load Profile

The load profile indicates the electricity usage pattern of consumers over time. To obtain an optimally configured HRES, the load profile needs to be accurate. Table 3 shows the load demand of a typical household in the study area, Hatiya. Daily demand for a single family is 12.088 kWh, which includes simple appliances appropriate for the rural low-income villagers. A hundred houses were considered, which makes the total energy consumption 120.88 kWh/day with a 14.95 kW peak demand. As a consequence, the load factor became 0.34. From 18.00 h to 21.00 h, demand was the highest, which was expected because; unlike the daytime during that period, the villagers tend to watch television and use lights.

Table 3. Energy consumption of a typical household in Hatiya.

Appliances	Power Rating (W)	Quantity	Daily Usage (Hours)
Lighting	10	3	10
Ceiling Fan	40	2	18
TV Set	80	1	10
Refrigerator	400	1	24
Mobile Charger	4	1	1.5

2.6. Solar Photovoltaic Module

The PV module generates DC electricity from sunlight. PV cells are the fundamental building block of PV modules. The output power of the PV module can be measured using the following Equation (11):

$$P_{PV} = Cp_{PV} * D_{PV}(\frac{Ir}{Ir_{STC}})[1 + \alpha_p(T_c) - T_{c,STC}] \quad (11)$$

The conditions for the standard test for calculating PV yield are 1 kW/m^2 of irradiation and a 25 °C cell temperature with the absence of wind. Typically, PV panel producers rate the generated power from the PV module at STCs, but in reality, this does not work this way because the sun temperature gets much higher than 25 °C.

Being a vital parameter for the PV system, PV efficiency refers to the ability of PV arrays to convert sunlight into DC electric power. The following equation can calculate the PV efficiency at the maximum power (MPP) and under STCs:

$$\eta_{STC} = \frac{Cp_{PV}}{A_{PV} * Ir_{STC}} \quad (12)$$

where η_{STC} denotes the efficiency of the PV module under standard test conditions (%) and A_{PV} stands for the surface area of the PV module (m^2).

It is worth noting that HOMER considers MPP efficiency the same as PV cell efficiency.

The renewable fraction (RF) of a system tells how much energy tapped from renewable sources actually serves the total electrical load demand per year. It is calculated by the following Equation (13):

$$F_{re} = 1 - \frac{E_{nonre}}{E_{served}} \quad (13)$$

Here, F_{re} is the renewable energy fraction (%); E_{nonre} stands for the total power (kWh/y) originated from non-renewable sources, which is the grid in this study; and E_{served} indicates the total electrical load served (kWh/y). Total grid electricity exports are also included in E_{served}.

For this study, a mono-crystalline solar module with passivated emitter and rear contact (PERC) technology is used. To intensify the aesthetics, these modules use a dark-colored back sheet and a black frame. The PV panel is assumed to be ground-mounted for every selected household. The detailed technical and economic parameters are shown in Table 4. The PV panel tilt angle and azimuth were set to 23.48° and 0°, suited for Bangladesh's weather [61].

Table 4. Component parameters.

Component	Manufacturer (Model)	Size (kW)	Lifetime (Years)	Cost ($)			Technical Parameters						Ref.
				Capital	O&M	Replacement	Derating Factor (%)	Panel Type	Ground Reflectance (%)	Temperature Coefficient (α_p)	NOCT (%/°C)	Efficiency (%)	
PV	Canadian Solar (CS6k-MS)	1	20	640	10	640	88	Flat plate	20	-0.390	45	17.72 @ STC	[14,62]
Converter	Leonics (S-219Cp)	1	20	600	10	600	-	-	-	-	-	96	[63]

2.7. Converter

Since the PV module has DC power output, while the grid supplies AC power, grid-connected HRES systems need power converters. It is a key component converting DC electricity to AC and vice versa. While serving AC electricity, the converters work as inverters. The rated power of the converter, P_{inv}, is the division of the peak load (P_{pk}) and inverter efficiency (η_{inv}) [64], as shown in the following Equation (14):

$$P_{inv} = \frac{P_{pk}}{\eta_{inv}} \tag{14}$$

In this study, we used a bidirectional grid-forming converter. It is capable of working on 220 volts (V) and 50 Hz frequency as required by the Bangladeshi utility and provides single-phase power output with the same voltage and frequency. In the case of a grid outage or disabled utility, the converter needs to be disconnected from the system and must be switched to islanded mode. The detailed technical and cost information is given in Table 4.

2.8. Economic Parameters

For conducting the economic analysis of a grid-tied PV project, the NPC and LCOE are the key elements. HOMER defines the net present cost (NPC) as the total annual cost during the whole project lifetime divided by the capital recovery factor (revenue that it receives over its lifetime). It is important because it is used to compute both the LCOE and NPC. The costs include capital cost, replacement cost, fuel cost, operation and maintenance cost, emission penalties, and the cost of buying power from the grid. Salvage income and grid sales earning are included in the revenue. The NPC can be calculated from the following equation [65]:

$$C_{npc} = \frac{C_{tot}}{R_f} \tag{15}$$

where C_{npc} = total annual cost ($/y), R_f = capital recovery factor, i= interest rate (%), and N = number of years.

However, the COE is calculated using the following mathematical formula [65].

$$COE = \frac{C_T}{E_{LS} + E_{grid}} \tag{16}$$

It divides the annualized cost of producing electricity (the total annualized cost minus the cost of serving the thermal load) by the total electric load served. Here, C_T is total annualized cost; E_{LS} is total load, both electrical (AC and DC) and thermal, that the MG actually serves. E_{grid} indicates total grid sales (kWh/y). It is worth noting that HOMER does not categorize the system configurations based on the COE, though it is convenient to do so; rather, it levels all system according to the NPC. This is because the value of the COE seems to be random, which is not the case of the NPC [65].

3. Results

3.1. PV Tracking

Though PV panels are normally mounted at a fixed orientation, which results in no tracking (NT), they can also be tracked to get maximum sunlight. When one axis performs the movement or adjustment of the surface, it is called single-axis solar tracking, and if the panel is adjusted with two axes simultaneously, it is called a dual-/two-axis tracking system (TA). Typically, there are five types of single-axis tracking, which are as follows [51]: (a) horizontal axis, monthly adjustment (HAM): horizontal east-west axis rotation and slope adjusted on the first day of every month; (b) horizontal axis, weekly adjustment (HAW): horizontal east-west axis rotation and slope adjusted on the first day of every week; (c) horizontal axis, daily adjustment (HAD): horizontal east-west axis rotation and slope adjusted each day; (d) horizontal axis, continuous adjustment (HAC): horizontal east-west axis rotation and slope adjusted regularly; (e) vertical axis, continuous adjustment (VAC): vertical axis rotation, slope fixed, and azimuth regularly adjusted.

In this study, all single-axis and two-axis tracking systems, along with no tracking were considered to find the best system in terms of the least NPC value. The input cost associated with the different trackers was adopted from [18]. Clearly, due to the absence of a tracker, the NT system has no tracker cost. The results in Figure 7 show that NT has

the lowest NPC, whereas the system has the highest NPC when TA tracking is installed. Therefore, NT is selected to perform further analysis.

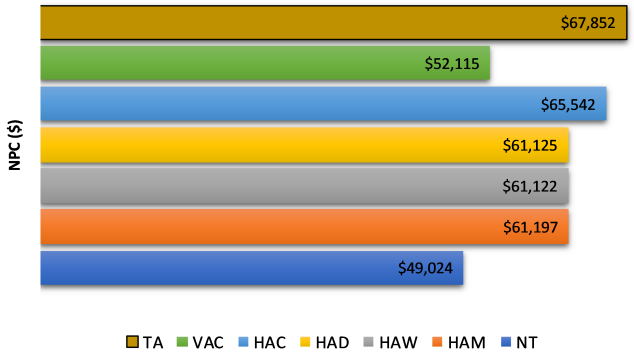

Figure 7. NPC of the system for different PV trackers. TA, dual-/two-axis tracking system; VAC, vertical axis, continuous adjustment; HAC, horizontal axis, continuous adjustment; HAD, horizontal axis, daily adjustment; HAW, horizontal axis, weekly adjustment; HAM, horizontal axis, monthly adjustment; NT, no tracking.

3.2. Performance of PV Systems Based on Derating Factor and Lifetime

Three PV derating factors (78%, 88%, and 98%) and two PV lifetime values (15 years and 20 years) were considered to understand their techno-economic impacts on the system. The combination of these two parameters results in six configurations: C1–C6. The technical and economic performance of all configurations are depicted in Table 5. Besides, Figure 8 shows the techno-economic effect of the three different values of the derating factor in terms of PV production and COE. A detailed analysis is carried out in the next two subsections. Here, C4 is taken as the reference case, and it is used to carry out the economic analysis for tracking systems in the previous section as well.

It should be mentioned that the ground reflectance was varied (20–40%) to perceive its influence on PV module, but all technical and economic result remained unchanged for all six designs. Therefore, it was concluded that the ground reflectance had very little to zero impact on the PV system for the selected study area.

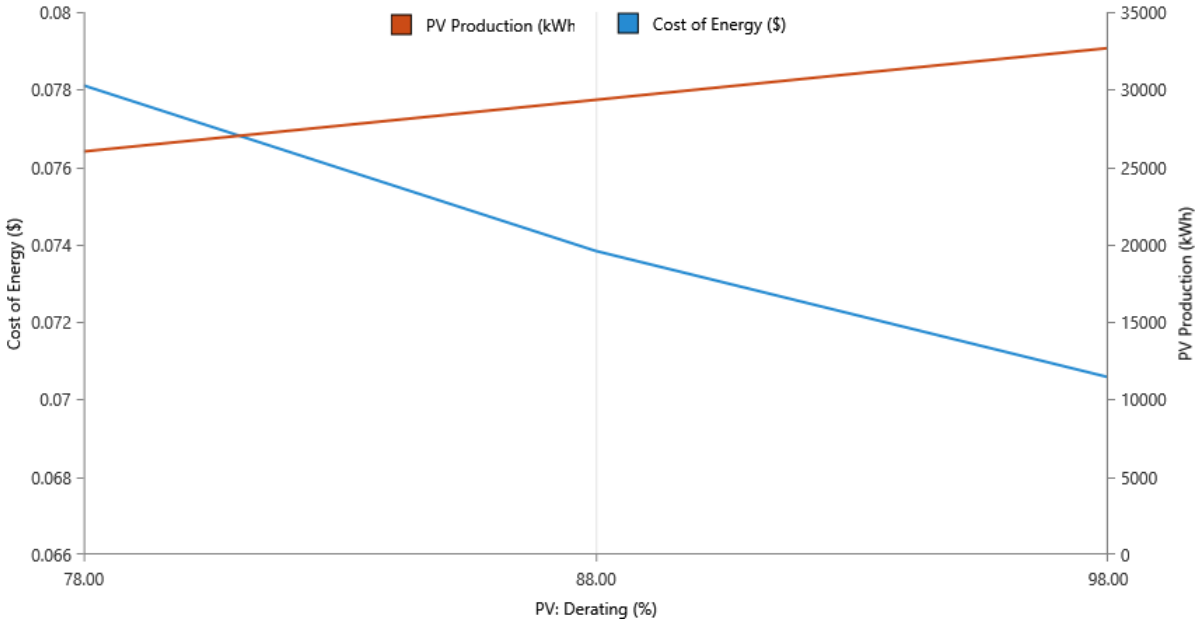

Figure 8. Techno-economic impact of different derating factors.

Table 5. Techno-economic performance parameters of different configurations.

Config.	PV Production (kWh)	PV Lifetime (Years)	PV Derating (%)	System COE ($)	System NPC ($)	System Operating Cost ($)	RE Fraction (%)	PV Capital Cost ($)	Grid Cost ($)	Grid Imports (kWh)	Grid Exports (kWh)
C1	26,006.54	15	78	0.0821	53,503.65	2684.479	33.769	12,800	23,127.61	33,370.68	6264.29
C2	26,006.54	20	78	0.0781	50,876.04	2481.222	33.769	12,800	23,127.61	33,370.68	6264.29
C3	29,340.71	15	88	0.0778	51,651.35	2541.196	37.355	12,800	21,275.30	32,174.84	7239.42
C4	29,340.71	20	88	0.0738	49,023.73	2337.938	37.355	12,800	21,275.30	32,174.84	7239.42
C5	32,674.89	15	98	0.0745	50,226.79	2431	39.976	12,800	19,850.75	31,313.18	8047.39
C6	32,674.89	20	98	0.0706	47,599.18	2227.743	39.976	12,800	19,850.75	31,313.18	8047.39

3.2.1. Technical Performance

A closer look at the configurations indicates that all of them met the load demand fully. Hence, there was no capacity shortage. In fact, they produced excess electricity and participated in exporting power to the grid. This was because of the significant power generation from the PV units, which contributed over 40% of the total system power output in each case. Since PV arrays operate during the daytime, the total running hours are 4373 throughout the year, which is around 12 h per day.

For the configurations C4 and C2, PV panels yielded 29,341 kWh per year (Figure 9), which is 47.7% of the total electricity production (61,516 kWh), while the rest of the electricity was purchased from the grid. Taking C4 as the base case, a ten percent change in the derating factor allowed the PV panels to increase and decrease the power generation by around 12% (3334 kWh) for C2 and C6, respectively, as shown in Table 5. Thus, it can be said that the rate of PV production was proportional to its derating factor. As we see from the monthly power generation point of view, this is also true. Despite low solar radiation from June to July in the study area of Hatiya (Figure 6), the PV output improved with the increased derating factors and vice versa. For example, in July, the PV modules of C2 produced 8 kW of power, whereas C6 produced 11 kW of power due to the higher derating factor.

Since solar production is only possible during the day while the most substantial amount of load demand occurs during the non-PV production hours, the excess electricity produced by the PV is tapped and sold to the grid later. Figure 10 represents a typical day of July, where the PV provides the highest power at noontime and consequently receives the highest excess electricity. It is evident that all load demand is met during that period by the PV panels only, and excess PV generation is sold to the grid. However, not all configurations provided the same amount of excess electricity, as well as grid import/import due to the different derating factors. C1 and C2 had the largest grid purchase (33,370 kWh/year) when the PV derating was the lowest (78%). At the same time, C5 and C6 experienced the smallest grid imports (31,313 kWh/year) when the derating factor was the highest (98%). The variation of excess PV power output from all configurations exhibited the same pattern as well.

By applying Equation (13), HOMER calculates the system RF. It should be noted that the RF is not the same as the total percentage of PV production because it does not count the excess electricity produced, but instead considers the actual RE (PV) penetration, which directly serves the load. The difference in the RF for each case can be seen in Figure 9. Here, C3 and C4 gained a 37.35% RF, whereas C1 and C2 had around 4% lower (33.76%) and C5 and C6 achieved approximately 3% higher RF (40%).

Figure 11 presents the cumulative distribution function (CDF) of different technical parameters based on the results of C4 on a daily basis. Although the cumulative frequency (CF) varied from 0-100% and 21–100% of total electrical load served and grid purchased electricity, respectively, the variation trend was almost the same because the system mostly received electricity from the grid. The PV module generated 65% to 100% surplus electricity,

which was not more than 17 kW per day, while the CF remained between 79% and 100% for the grid sales, implying less than 9 kW of power was exported to the grid.

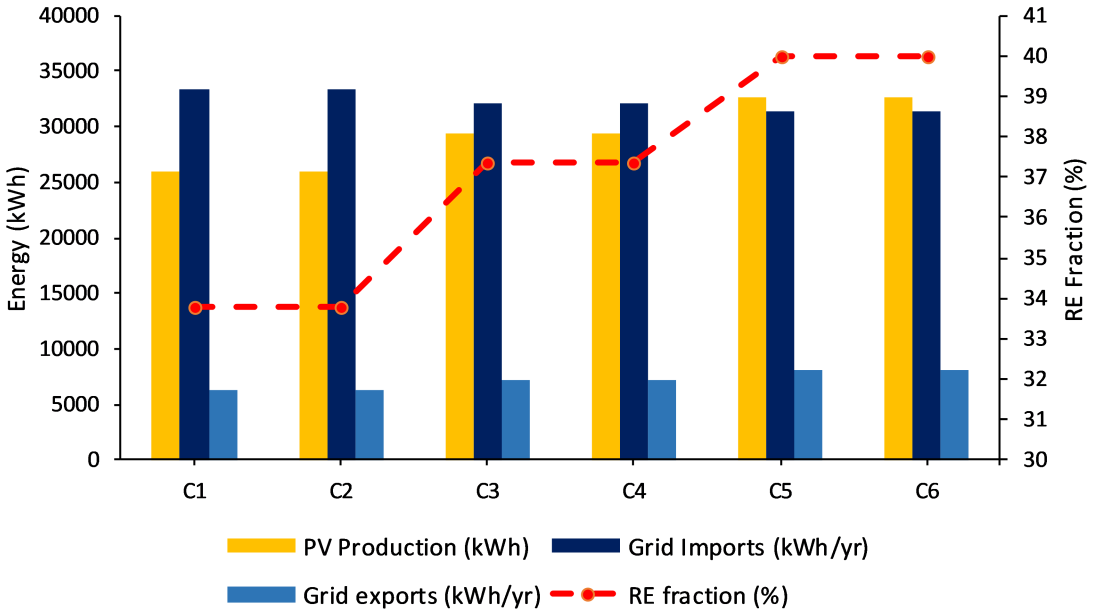

Figure 9. Electrical output parameters of various configurations.

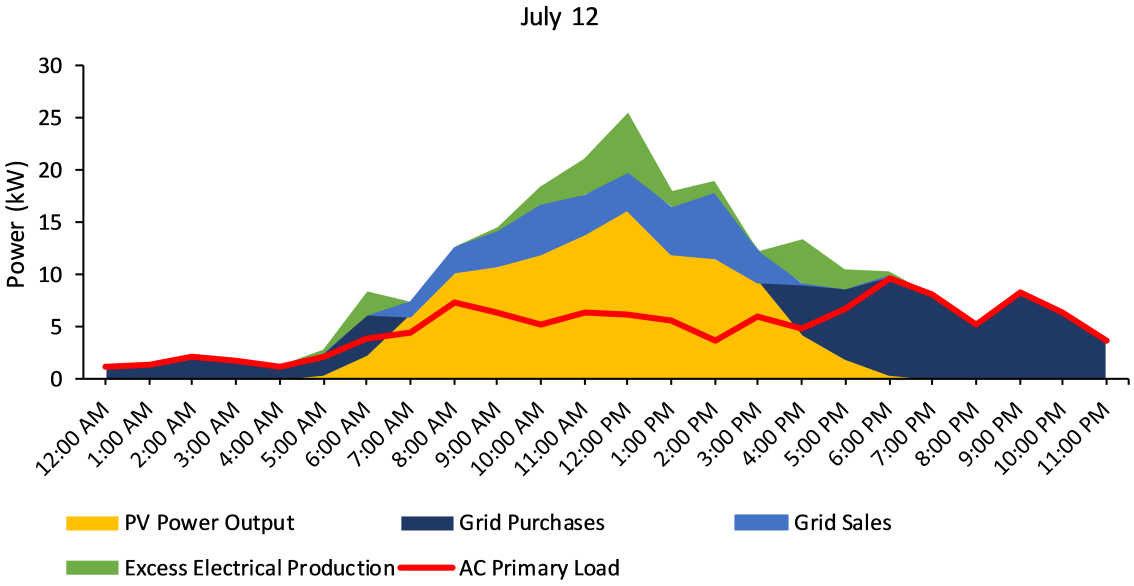

Figure 10. PV output power performance with respect to total electrical load served, excess electricity, and grid sales.

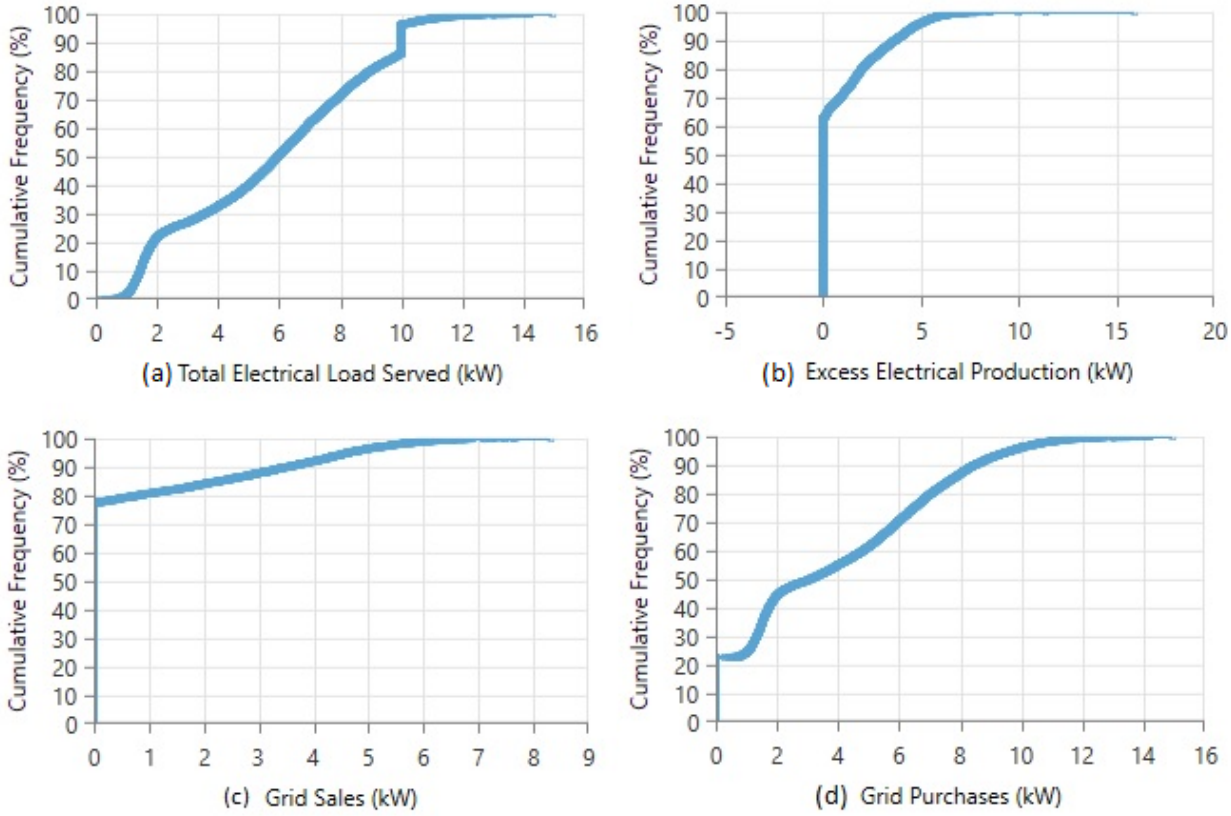

Figure 11. Cumulative distribution function of (**a**) total load served, (**b**) excess electricity, (**c**) grid sales, and (**d**) grid purchase.

3.2.2. Economic Performance

In general, the grid was the most costly component among all six cases, and the converter had the least cost. Clearly, the system had the largest cost for operation owing to the grid purchase, followed by the capital, replacement, and salvage cost. Because of the absence of non-renewable sources, there was no fuel cost. A sample cost summary of the C4 scenario is presented in Figure 12. The total NPC was $49,023.74, where grid, PV, and converter had shares of 43%, 22%, and 35%, respectively. The NPC and operating cost of the C4 case were responsible for $0.0738 of the system COE per kWh, as shown in Table 5.

Figure 13 represents various costs associated with different system designs. The comparative analysis between all scenarios demonstrates that C1 had the highest cost, while C6 had the least cost in terms of all types of costs. This is because of the lowest PV lifetime (15 years) and derating factor (78%) of C1 and the highest PV lifetime (20 years) and derating factor (98%) of C6. A ten percent deviation of the derating factor from the base case elevated the NPC to around 4% ($1852/kWh) for C2, alternatively reducing the NPC by about 3% ($1424/kWh) for C6. This result suggests that the system obtains lower costs with the improvement of the derating factor. However, the PV lifetime also affects the system cost, and it did not exhibit the same pattern as PV electricity production. Taking C3 and C4 as examples, it is noticed that both cases produced the same PV electricity and consequently had the same electric export/import and RF, but possessed different costs (NPC, COE, and operating cost). The NPC reduced by around $2628 due to the five years of difference in the PV lifetime considering the same derating factor (88%). Again, the grid cost had an equal value because the system imported the same amount of electricity from the grid.

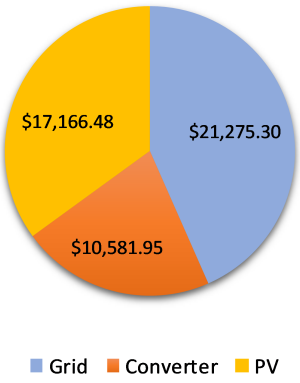

Figure 12. Net present cost summary of the C4 PV system.

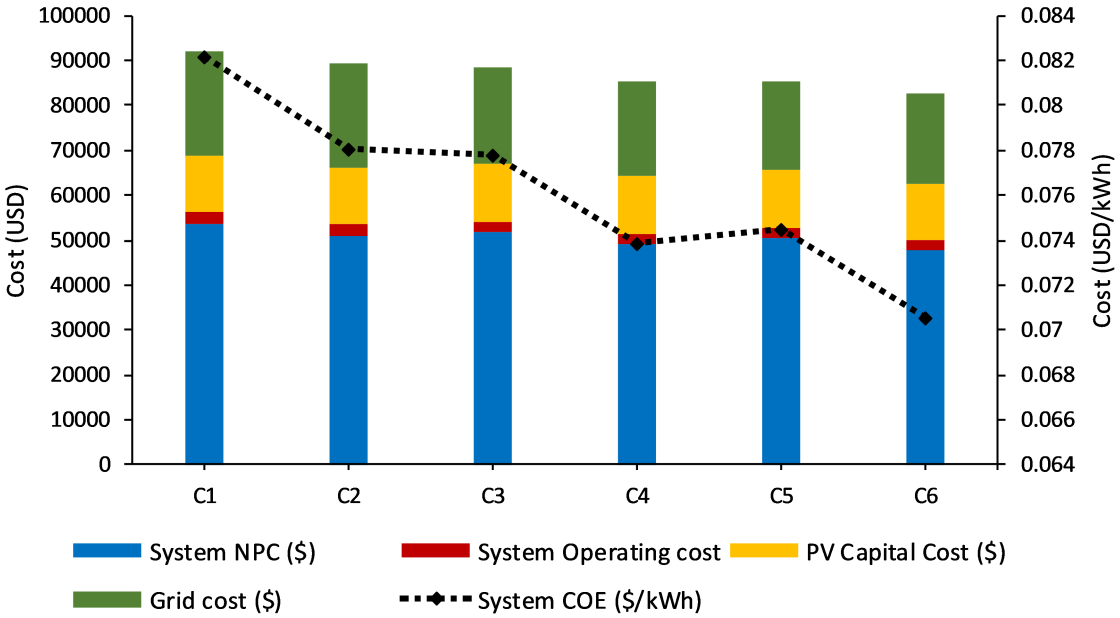

Figure 13. Cost breakdown for different designs.

3.3. Impact of Degradation on PV Systems

The base case C4 was selected to observe the impact of degradation/aging on this grid-connected PV system. According to the Bangladeshis government rule, solar PV modules must be guaranteed for at least 20 years and should encounter a maximum of a twenty percent reduction in their yield over their lifetime [61]. However, a period of 20 years with a median degradation rate of 0.5%/year [53,66] was chosen as the HOMER input. Though degradation is a part of the derating factor, it is worth noting that HOMER does not include this parameter in the derating factor, rather considering it a separate indicator with multi-year mode.

The multi-year simulation result is shown in Figure 14. Obviously, electrical output from aged PV panels declines over the years, while the levelized cost of PV panels and net energy import from the grid increased. In twenty years, PV power generation would reduce by 2665 kWh, which is around 10% from the first year. Similarly, To produce 1 kWh of electricity, the cost of the PV modules would be almost 9% ($0.045/kWh to $0.049/kWh) higher at the end of the 20th year. It goes without saying that different costs such as the NPC, system COE, and operating cost will also become larger. Over the years, the system

would be more grid dependent, and grid exports would be lower owing to the lower PV production.

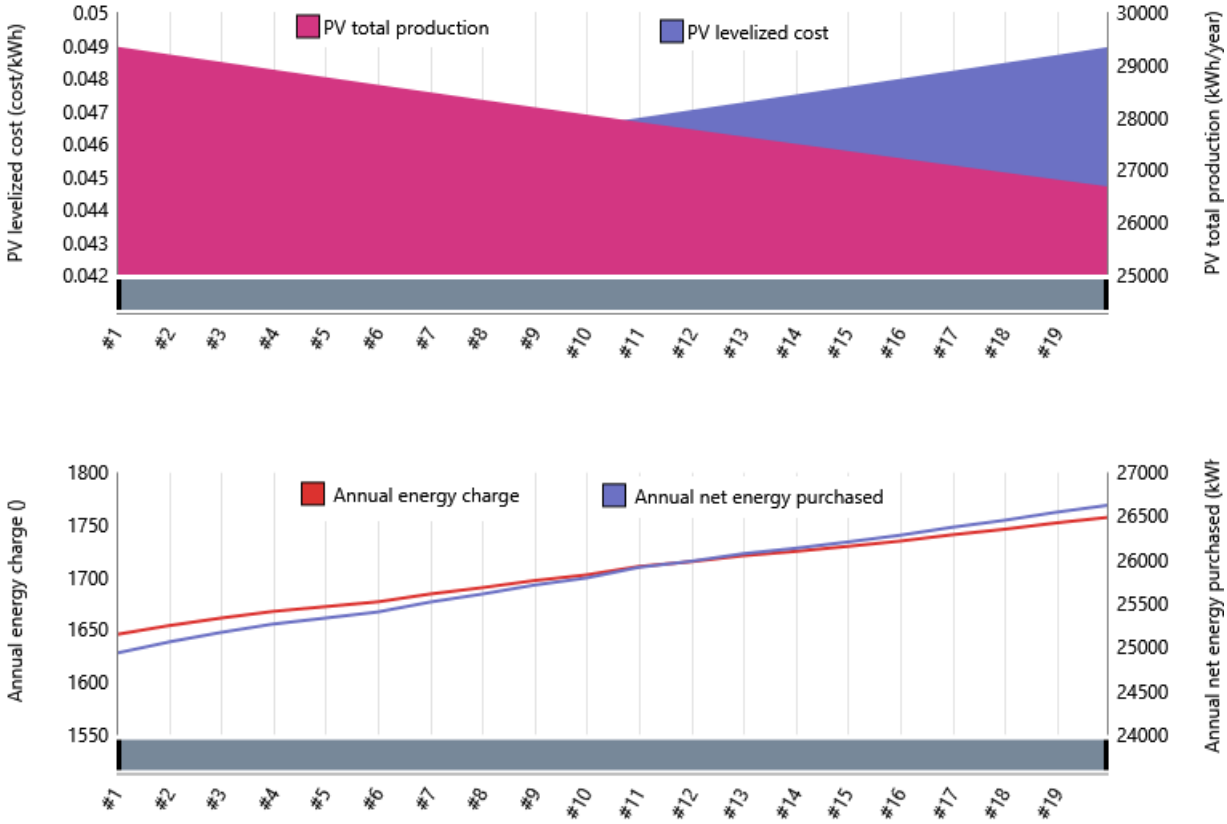

Figure 14. Effect of PV degradation: (**a**) PV production vs. PV levelized cost and (**b**) annual energy charge vs. net energy purchased.

3.4. Impact of Ambient Temperature

Ambient temperature (T_a) refers to the air temperature of the environment surrounding any particular area. It is used to measure the PV cell temperature (T_c), which is a major criterion that affects the PV derating factor, as indicated in Equation (1). Hence, the variation of T_a influences the PV productivity. As a consequence, the economic value of the PV project also is affected. In view of base case C4, Figure 15 represents the impact of different ambient temperatures on PV yield and system COE, whereas Figure 16 shows the impact of PV lifetime and temperature on PV production with the system NPC superimposed.

From the figures, it is clear that with the rise of ambient temperature, PV electricity declines, which leads to the escalation of the whole system cost. At an average annual T_a of 25.4 °C, C4 produces 29,341 kWh of electricity with a per kWh energy cost of $0.078. When T_a decreases to 20 °C, the PV panel produces 675 kWh more electricity (30,016 kWh) and saves 0.007 ($/kWh) in the cost of energy. On the contrary, the PV panel yields 580 kWh less electricity, and the system loses 0.008 ($/kWh) in the COE when T_a rises to 30 °C. The NPC also follows the same trend as the COE with the variation in the average temperature. A closer look at the results shows that the rate of change of both PV generation and the COE is higher at 30 °C compared to the case when T_a is 20 °C. These results support the fact that a higher ambient temperature lessens the PV panel's efficiency, which leads to economic loss.

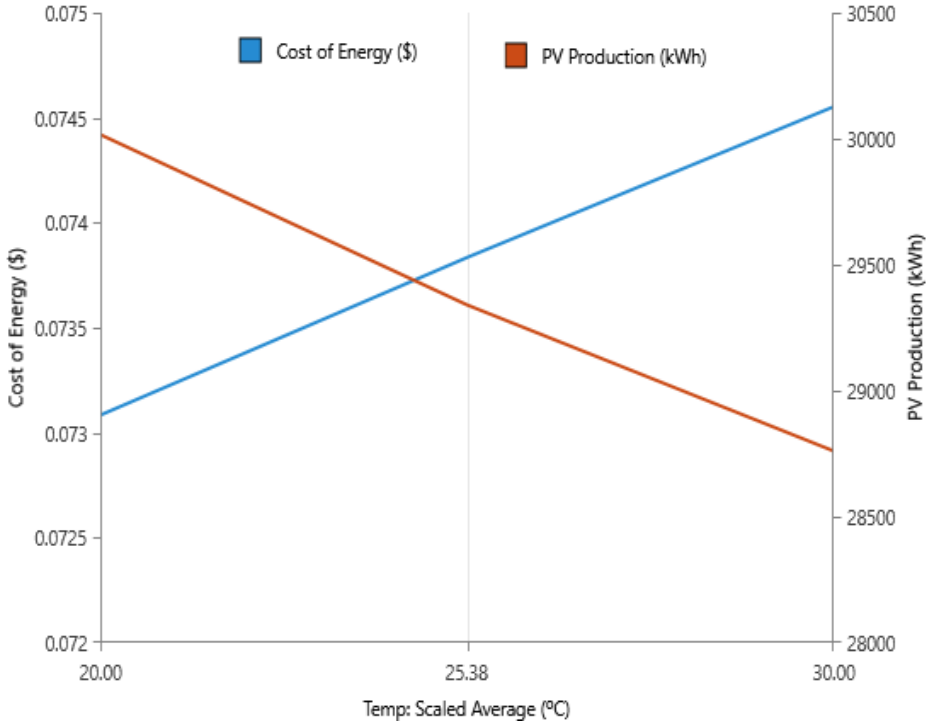

Figure 15. Effect of ambient temperature on PV production and system COE.

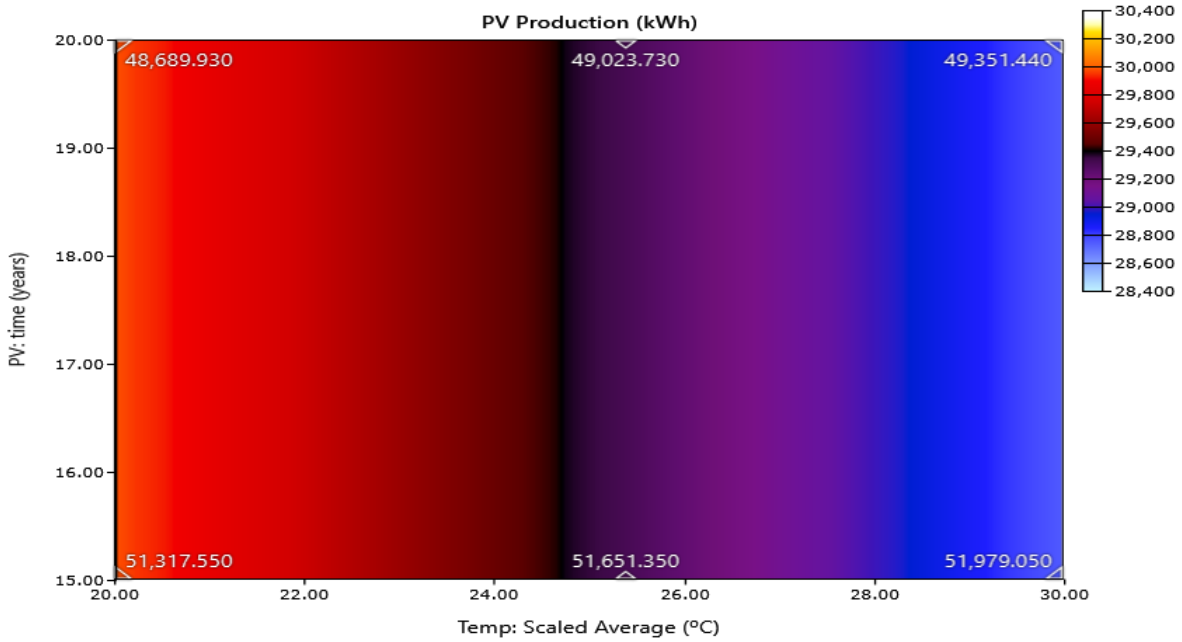

Figure 16. Effect of PV lifetime and ambient temperature on PV production and system NPC.

4. Conclusion and Future Works

Precise understanding of the impact of the derating factor is pivotal to the continued growth of the PV industry as it sets the investor's perception of PV performance and net economic return. A mathematical model is presented to calculate the optimum angle based on the annual average solar irradiation of the PV panel located in the study site. The economic viability of PV tracker installation is analyzed as well. It is observed that there is a 1.02 kWh/m^2/day increase in solar radiation subject to the adoption of the optimal tilt angle, and the PV system is better off without any trackers given the cost of the

tracking system. As the existing literature lacks a discussion of the combined impact of such parameters, we investigate the technical and financial effects of varying the derating factor on the grid-tied PV system in this study. Results illustrate that the PV module tends to produce more output power with a reduced associated economic cost when the PV derating factor decreases and vice versa. Variation in the derating factor also affects the export/import from and to the grid in the same manner. Two parameters affiliated with the derating factor—degradation and ambient temperature—are considered separately to observe their techno-economic impact. At a 0.5% degradation rate and a 20 year lifespan, the PV module produces 10% less electricity in the last year compared to the starting year, which leads to a 9% rise in the per-unit cost of energy. From the comparative analysis for the case of Hatiya, it is found that the PV module output reduces (produces 580 kWh less electricity at 30 °C than at 24.5 °C) due to the higher PV cell temperature accompanied by the ambient temperature. As a consequence, the system cost increases.

To conclude, this study intends to assist PV designers and investors in pondering the effects of derating factors and planning their projects accordingly. For further research, comparative performance analysis can be done between off-grid and grid-connected PV designs in terms of the derating factor, PV degradation, and lifetime, along with other parameters.

Supplementary Materials: The following are available online at https://www.mdpi.com/1996-1073/14/4/1044/s1; Characterization in using optimum tilt angle and description of an actual and forecasted photovoltaic power output.

Author Contributions: Conceptualization, H.M.; methodology, H.M.; software, H.M.; validation, H.M. and K.V.K.; formal analysis, H.M. and M.A.; investigation, H.M.; resources, H.M.; data curation, H.M.; writing—original draft preparation, H.M.; writing—review and editing, H.M., K.V.K., M.A., M.L.O. and K.R.K.; visualization, H.M.; supervision, T.S.; project administration, H.M.; funding acquisition, T.S. All authors have read and agreed to the published version of the manuscript.

Funding: This research received no external funding.

Institutional Review Board Statement: Not applicable.

Informed Consent Statement: Not applicable.

Data Availability Statement: Data is available upon request.

Conflicts of Interest: The authors declare no conflict of interest.

References

1. Renewables Global Status Report—REN21. 2019. Available online: https://www.ren21.net/reports/global-status-report/ (accessed on 6 September 2020).
2. Future of Solar Photovoltaic—IRENA. 2019. Available online: https://www.irena.org/-/media/Files/IRENA/Agency/Publication/2019/Nov/IRENA_Future_of_Solar_PV_2019.pdf (accessed on 8 October 2020).
3. Dobos, A.P. *PVWatts Version 5 Manual*; Technical Report; National Renewable Energy Lab. (NREL): Golden, CO, USA, 2014.
4. Marion, B.; Adelstein, J.; Boyle, K.; Hayden, H.; Hammond, B.; Fletcher, T.; Canada, B.; Narang, D.; Kimber, A.; Mitchell, L.; et al. Performance Parameters for Grid-Connected PV Systems. In Proceedings of the Conference Record of the Thirty-first IEEE Photovoltaic Specialists Conference, Lake Buena Vista, FL, USA, 3–7 January 2005. [CrossRef]
5. Lau, K.Y.; Tan, C.W.; Yatim, A.H.M. Effects of ambient temperatures, tilt angles, and orientations on hybrid photovoltaic/diesel systems under equatorial climates. *Renew. Sustain. Energy Rev.* **2018**, *81*, 2625–2636. [CrossRef]
6. Ullah, A.; Imran, H.; Maqsood, Z.; Butt, N.Z. Investigation of optimal tilt angles and effects of soiling on PV energy production in Pakistan. *Renew. Energy* **2019**, *139*, 830–843. [CrossRef]
7. Yerli, B.; Kaymak, M.K.; İzgi, E.; Öztopal, A.; Şahin, A.D. Effect of derating factors on photovoltaics under climatic conditions of Istanbul. *World Acad. Sci. Eng. Technol.* **2010**, *44*, 1400–1404.
8. Appels, R.; Lefevre, B.; Herteleer, B.; Goverde, H.; Beerten, A.; Paesen, R.; De Medts, K.; Driesen, J.; Poortmans, J. Effect of soiling on photovoltaic modules. *Sol. Energy* **2013**, *96*, 283–291. [CrossRef]
9. Cordero, R.R.; Damiani, A.; Laroze, D.; MacDonell, S.; Jorquera, J.; Sepúlveda, E.; Feron, S.; Llanillo, P.; Labbe, F.; Carrasco, J.; et al. Effects of soiling on photovoltaic (PV) modules in the Atacama Desert. *Sci. Rep.* **2018**, *8*, 1–14. [CrossRef]
10. Lopez-Garcia, J.; Pozza, A.; Sample, T. Long-term soiling of silicon PV modules in a moderate subtropical climate. *Sol. Energy* **2016**, *130*, 174–183. [CrossRef]
11. Maghami, M.R.; Hizam, H.; Gomes, C.; Radzi, M.A.; Rezadad, M.I.; Hajighorbani, S. Power loss due to soiling on solar panel: A review. *Renew. Sustain. Energy Rev.* **2016**, *59*, 1307–1316. [CrossRef]

12. Hocine, L.; Mounia Samira, K. Optimal PV panel's end-life assessment based on the supervision of their own aging evolution and waste management forecasting. *Sol. Energy* **2019**, *191*, 227–234. [CrossRef]
13. Rahman, M.M.; Islam, M.A.; Karim, A.H.M.Z.; Ronee, A.H. Effects of Natural Dust on the Performance of PV Panels in Bangladesh, 2019. Available online: http://www.mecs-press.org/ijmecs/ijmecs-v4-n10/v4n10-4.html (accessed on 16 November 2019).
14. Al Garni, H.Z.; Awasthi, A.; Ramli, M.A.M. Optimal design and analysis of grid-connected photovoltaic under different tracking systems using HOMER. *Energy Convers. Manag.* **2018**, *155*, 42–57. [CrossRef]
15. Shabani, M.; Mahmoudimehr, J. Techno-economic role of PV tracking technology in a hybrid PV-hydroelectric standalone power system. *Appl. Energy* **2018**, *212*, 84–108. [CrossRef]
16. Ilse, K.; Micheli, L.; Figgis, B.W.; Lange, K.; Daßler, D.; Hanifi, H.; Wolfertstetter, F.; Naumann, V.; Hagendorf, C.; Gottschalg, R.; et al. Techno-Economic Assessment of Soiling Losses and Mitigation Strategies for Solar Power Generation. *Joule* **2019**, *3*, 2303–2321. [CrossRef]
17. Song, Z.; McElvany, C.L.; Phillips, A.B.; Celik, I.; Krantz, P.W.; Watthage, S.C.; Liyanage, G.K.; Apul, D.; Heben, M.J. A technoeconomic analysis of perovskite solar module manufacturing with low-cost materials and techniques. *Energy Environ. Sci.* **2017**, *10*, 1297–1305. [CrossRef]
18. Sinha, S.; Chandel, S.S. Analysis of fixed tilt and sun tracking photovoltaic–micro wind based hybrid power systems. *Energy Convers. Manag.* **2016**, *115*, 265–275. [CrossRef]
19. Quansah, D.A.; Adaramola, M.S. Ageing and degradation in solar photovoltaic modules installed in northern Ghana. *Sol. Energy* **2018**, *173*, 834–847. [CrossRef]
20. Tanesab, J.; Parlevliet, D.; Whale, J.; Urmee, T. Energy and economic losses caused by dust on residential photovoltaic (PV) systems deployed in different climate areas. *Renew. Energy* **2018**, *120*, 401–412. [CrossRef]
21. You, S.; Lim, Y.J.; Dai, Y.; Wang, C.H. On the temporal modelling of solar photovoltaic soiling: Energy and economic impacts in seven cities. *Appl. Energy* **2018**, *228*, 1136–1146. [CrossRef]
22. Micheli, L.; Fernández, E.F.; Aguilera, J.T.; Almonacid, F. Economics of seasonal photovoltaic soiling and cleaning optimization scenarios. *Energy* **2021**, *215*, 119018. [CrossRef]
23. Malvoni, M.; Kumar, N.M.; Chopra, S.S.; Hatziargyriou, N. Performance and degradation assessment of large-scale grid-connected solar photovoltaic power plant in tropical semi-arid environment of India. *Sol. Energy* **2020**, *203*, 101–113. [CrossRef]
24. Limmanee, A.; Songtrai, S.; Udomdachanut, N.; Kaewniyompanit, S.; Sato, Y.; Nakaishi, M.; Kittisontirak, S.; Sriprapha, K.; Sakamoto, Y. Degradation analysis of photovoltaic modules under tropical climatic conditions and its impacts on LCOE. *Renew. Energy* **2017**, *102*, 199–204. [CrossRef]
25. Jordan, D.C.; Kurtz, S.R.; VanSant, K.; Newmiller, J. Compendium of photovoltaic degradation rates. *Prog. Photovoltaics Res. Appl.* **2016**, *24*, 978–989. [CrossRef]
26. Theristis, M.; Livera, A.; Jones, C.B.; Makrides, G.; Georghiou, G.E.; Stein, J.S. Nonlinear Photovoltaic Degradation Rates: Modeling and Comparison Against Conventional Methods. *IEEE J. Photovoltaics* **2020**, *10*, 1112–1118. [CrossRef]
27. Micheli, L.; Theristis, M.; Talavera, D.L.; Almonacid, F.; Stein, J.S.; Fernández, E.F. Photovoltaic cleaning frequency optimization under different degradation rate patterns. *Renew. Energy* **2020**, *166*, 136–146. [CrossRef]
28. California Energy Commission. A guide to photovoltaic (PV) system design and installation. *Endecon Eng.* **2001**, *347*, 4–10.
29. Enphase Microinverters | Enphase Microinverter Solar Systems Geelong. 2020. Available online: https://enphase.com/en-in (accessed on 12 September 2020).
30. Alam Hossain Mondal, Md.; Sadrul Islam, A.K.M. Potential and viability of grid-connected solar PV system in Bangladesh. *Renew. Energy* **2011**, *36*, 1869–1874. [CrossRef]
31. Islam, A.; Shima, F.A.; Khanam, A. Analysis of grid connected solar PV system in the southeastern part of Bangladesh. *Appl. Sol. Energy* **2013**, *49*, 116–123. [CrossRef]
32. Shuvho, M.B.A.; Chowdhury, M.A.; Ahmed, S.; Kashem, M.A. Prediction of solar irradiation and performance evaluation of grid connected solar 80KWp PV plant in Bangladesh. *Energy Rep.* **2019**, *5*, 714–722. [CrossRef]
33. Sarkar, Md.N.I.; Ghosh, H.R. Techno-economic analysis and challenges of solar powered pumps dissemination in Bangladesh. *Sustain. Energy Technol. Assess.* **2017**, *20*, 33–46. [CrossRef]
34. Li, C.; Ge, X.; Zheng, Y.; Xu, C.; Ren, Y.; Song, C.; Yang, C. Techno-economic feasibility study of autonomous hybrid wind/PV/battery power system for a household in Urumqi, China. *Energy* **2013**, *55*, 263–272. [CrossRef]
35. Kumar, N.M.; Vishnupriyan, J.; Sundaramoorthi, P. Techno-economic optimization and real-time comparison of sun tracking photovoltaic system for rural healthcare building. *J. Renew. Sustain. Energy* **2019**, *11*, 015301. [CrossRef]
36. Vishnupriyan, J.; Manoharan, P.S. Prospects of hybrid photovoltaic–diesel standalone system for six different climate locations in Indian state of Tamil Nadu. *J. Clean. Prod.* **2018**, *185*, 309–321. [CrossRef]
37. Khatib, T.; Mohamed, A.; Sopian, K. Optimization of a PV/wind micro-grid for rural housing electrification using a hybrid iterative/genetic algorithm: Case study of Kuala Terengganu, Malaysia. *Energy Build.* **2012**, *47*, 321–331. [CrossRef]
38. Sharma, H.; Mishra, S. Techno-economic analysis of solar grid-based virtual power plant in Indian power sector: A case study. *Int. Trans. Electr. Energy Syst.* **2019**, *30*, e12177. [CrossRef]
39. Jung, J.; Villaran, M. Optimal planning and design of hybrid renewable energy systems for microgrids. *Renew. Sustain. Energy Rev.* **2017**, *75*, 180–191. [CrossRef]

40. Guinot, B.; Champel, B.; Montignac, F.; Lemaire, E.; Vannucci, D.; Sailler, S.; Bultel, Y. Techno-economic study of a PV-hydrogen-battery hybrid system for off-grid power supply: Impact of performances' aging on optimal system sizing and competitiveness. *Int. J. Hydrogen Energy* **2015**, *40*, 623–632. [CrossRef]
41. Hossain, M.; Mekhilef, S.; Olatomiwa, L. Performance evaluation of a stand-alone PV-wind-diesel-battery hybrid system feasible for a large resort center in South China Sea, Malaysia. *Sustain. Cities Soc.* **2017**, *28*, 358–366. [CrossRef]
42. Abdilahi, A.M.; Mohd Yatim, A.H.; Mustafa, M.W.; Khalaf, O.T.; Shumran, A.F.; Mohamed Nor, F. Feasibility study of renewable energy-based microgrid system in xn–Somalilands-uxn urban centers. *Renew. Sustain. Energy Rev.* **2014**, *40*, 1048–1059. [CrossRef]
43. Mao, M.; Jin, P.; Chang, L.; Xu, H. Economic Analysis and Optimal Design on Microgrids With SS-PVs for Industries. *IEEE Trans. Sustain. Energy* **2014**, *5*, 1328–1336. [CrossRef]
44. Ishaque, K.; Salam, Z.; Amjad, M.; Mekhilef, S. An Improved Particle Swarm Optimization (PSO)–Based MPPT for PV With Reduced Steady-State Oscillation. *IEEE Trans. Power Electron.* **2012**, *27*, 3627–3638. [CrossRef]
45. Kaur, R.; Krishnasamy, V.; Kandasamy, N.K. Optimal sizing of wind–PV-based DC microgrid for telecom power supply in remote areas. *IET Renew. Power Gener.* **2018**, *12*, 859–866. [CrossRef]
46. Kornelakis, A.; Koutroulis, E. Methodology for the design optimisation and the economic analysis of grid-connected photovoltaic systems. *IET Renew. Power Gener.* **2009**, *3*, 476–492. [CrossRef]
47. Ma, W.; Fan, J.; Fang, S.; Liu, G. Techno-economic potential evaluation of small-scale grid-connected renewable power systems in China. *Energy Convers. Manag.* **2019**, *196*, 430–442. [CrossRef]
48. Sinha, S.; Chandel, S.S. Review of software tools for hybrid renewable energy systems. *Renew. Sustain. Energy Rev.* **2014**, *32*, 192–205. [CrossRef]
49. Masrur, H.; Howlader, H.O.R.; Elsayed Lotfy, M.; Khan, K.R.; Guerrero, J.M.; Senjyu, T. Analysis of Techno-Economic-Environmental Suitability of an Isolated Microgrid System Located in a Remote Island of Bangladesh. *Sustainability* **2020**, *12*, 2880. [CrossRef]
50. Gevorkian, P. Grid-Connected Photovoltaic Power Generation by Peter Gevorkian. *Camb. Core* **2017**, 7–34. [CrossRef]
51. HOMER Pro User Manual. 2019. Available online: https://www.homerenergy.com/products/pro/docs/3.10/index.html (accessed on 10 December 2019).
52. Akinyele, D. Techno-economic design and performance analysis of nanogrid systems for households in energy-poor villages. *Sustain. Cities Soc.* **2017**, *34*, 335–357. [CrossRef]
53. Jordan, D.C.; Kurtz, S.R. Photovoltaic Degradation Rates—an Analytical Review. *Prog. Photovoltaics Res. Appl.* **2013**, *21*, 12–29. [CrossRef]
54. Monocrystalline vs. Polycrystalline Solar Panels|EnergySage. 2020. Available online: https://www.energysage.com/solar/101/monocrystalline-vs-polycrystalline-solar-panels/ (accessed on 2 September 2020).
55. Performance Analysis of PV Cells under Monsoon Climate. 2020. Available online: https://www.researchgate.net/publication/331864280_Performance_Analysis_of_PV_Cells_under_Monsoon_Climate (accessed on 4 September 2020).
56. Climate Chittagong Division: Temperature, Climate Graph, Climate Table. 2021. Available online: https://en.climate-data.org/asia/bangladesh/chittagong-division-2276/ (accessed on 3 February 2020).
57. Yadav, A.K.; Malik, H. Optimization of Tilt Angle for Intercepting Maximum Solar Radiation for Power Generation. In *Optimization of Power System Problems*; Springer: Berlin/Heidelberg, Germany, 2020; pp. 195–213.
58. Masrur, H.; Othman, M.L.; Arefin, A.A.; Hizam, H.B.; Wahab, N.I.A.; Islam, S.Z.; Senjyu, T. Determining Optimal Tilt Angle to Maximize the PV Yield. In Proceedings of the 2020 IEEE International Conference on Power and Energy (PECon), Penang, Malaysia, 7–8 December 2020; pp. 219–223. [CrossRef]
59. NREL-NSRDB Data Viewer. 2019. Available online: https://maps.nrel.gov/nsrdb-viewer/ (accessed on 13 October 2020).
60. Chowdhury, N.; Hossain, C.A.; Longo, M.; Yaïci, W. Optimization of Solar Energy System for the Electric Vehicle at University Campus in Dhaka, Bangladesh. *Energies* **2018**, *11*, 2433. [CrossRef]
61. Technical Standards for IDCOL Solar Home Systems Program. 2019. Available online: https://idcol.org/home/downloads (accessed on 14 December 2019).
62. Datasheet, Canadian Solar. 2020. Available online: https://www.csisolar.com/downloads/ (accessed on 2 September 2020).
63. LEONICS Inverter S-210 Series. 2020. Available online: http://www.leonics.com/product/renewable/inverter/inverter_apollo_s-210_en.php (accessed on 2 October 2020).
64. Javed, M.S.; Song, A.; Ma, T. Techno-economic assessment of a stand-alone hybrid solar-wind-battery system for a remote island using genetic algorithm. *Energy* **2019**, *176*, 704–717. [CrossRef]
65. Lambert, T.; Gilman, P.; Lilienthal, P. Micropower system modeling with HOMER. *Integr. Altern. Sources Energy* **2006**, *1*, 379–385.
66. Imam, A.A.; Al-Turki, Y.A. Techno-Economic Feasibility Assessment of Grid-Connected PV Systems for Residential Buildings in Saudi Arabia—A Case Study. *Sustainability* **2020**, *12*, 262. [CrossRef]